# Anisole hydrodeoxygenation over nickel-based catalysts

Yusuf, Mustapha; Leeke, Gary; Wood, Joe

*DOI:*
10.1021/acs.energyfuels.2c03734



*Document Version*
Publisher's PDF, also known as Version of record

*Citation for published version (Harvard):*
Yusuf, M, Leeke, G & Wood, J 2023, 'Anisole hydrodeoxygenation over nickel-based catalysts: influence of solvent and support properties', *Energy & Fuels*, vol. 37, no. 2, pp. 1225-1237. https://doi.org/10.1021/acs.energyfuels.2c03734

energy&fuels

pubs.acs.org/EF

Article

# Anisole Hydrodeoxygenation over Nickel-Based Catalysts: Influences of Solvent and Support Properties

Mustapha Yusuf, Gary Leeke, and Joseph Wood*

Cite This: https://doi.org/10.1021/acs.energyfuels.2c03734

Read Online

ACCESS | Metrics & More | Article Recommendations | Supporting Information

**ABSTRACT:** The realization of biofuels and chemicals requires the development of highly active and selective catalysts, which are resistant to deactivation. A conventional ZSM-5 ($SiO_2/Al_2O_3$ = 30) was modified with 0.2 M NaOH to generate a mesoporous zeolite support. The parent zeolite, mic-ZSM-5, the modified zeolite, hie-ZSM-5, and a mesoporous silica support, $SiO_2$, were impregnated with 5% nickel and characterized using X-ray powder diffraction (XRD), Brunauer−Emmett−Teller (BET) analysis of nitrogen sorption, scanning electron microscopy with energy dispersive X-ray (SEM-EDX), transmission electron microscopy (TEM), hydrogen temperature-programmed reduction ($H_2$-TPR), ammonium hydrogen temperature-programmed desorption ($NH_3$-TPD), and thermogravimetric analysis (TGA). The influences of the support properties and solvent during the hydrodeoxygenation of anisole were investigated by measuring concentration profiles and rates in a high-pressure batch reactor. NaOH treatment significantly improved the pore structure, acidity of the support, and metal dispersion as well as the interaction of nonframework Ni species with zeolite and, hence, the catalytic activity and selectivity. The highest anisole conversion of 100% was obtained in 120 min over the hie-Ni/ZSM-5 catalyst with cyclohexane selectivity of 88.1%. In addition, the Ni/$SiO_2$ catalyst was 84.5% selective to toluene at 48.9% anisole conversion in 120 min; as such, it was proposed that the transformation of anisole proceeds via either a direct deoxygenation−hydrogenation or isomerization−direct deoxygenation pathway. However, no substantial differences in anisole conversion or product selectivity were observed when decalin and *n*-decane were compared as solvents. A catalyst reusability test showed hie-Ni/ZSM-5 as the most stable of the three catalysts in terms of anisole transformation, even though the catalyst recorded the biggest weight loss of 9.2% suggesting high resistance to carbon deactivation. Therefore, with this very good catalytic activity, good selectivity to liquid product, and stability, the mesoporous Ni/ZSM-5 catalyst is a potential candidate for economically beneficial future industrial applications.

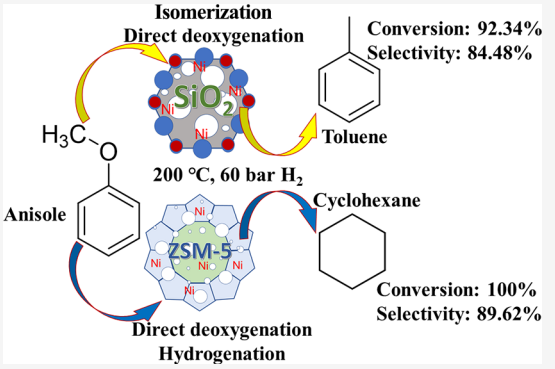




## 1. INTRODUCTION

Significant efforts are being made to develop renewable energy sources in order to address the rising demand for energy as well as the environmental and socio-political challenges brought on by the existing heavy reliance on fossil fuels worldwide.[1] Biomass is a reliable alternative raw material from which to manufacture chemicals, is generally believed to be more environmentally benign, and also has the potential to provide sustainable sources of energy.[2] Unlike fossil fuels, biomass-derived fuel such as bio-oil is renewable, provided it is derived from sustainable sources.[3,4] Unfortunately, bio-oil has a number of limitations because of its high viscosity, high oxygen content, and complex chemical composition. This results in low quality fuel and incompatibility with existing industrial facilities and current transportation infrastructure,[5,6] hence, the need for upgrading.[7,8] Upgrading technology focuses on enhancing the quality and compatibility of bio-oil to generate market-driven biofuels and biochemicals.[5] An efficient chemical route for upgrading bio-oil is catalytic hydrodeoxygenation (HDO).[9] The aims of HDO are to improve the heating value, increase stability, and enhance miscibility with conventional fuels, thereby decreasing the viscosity and corrosiveness. These are normally achieved via hydrogenolysis of C−O bonds, which subsequently remove oxygen in the form of water.[5,10]

Different catalysts have been prepared and used for the HDO reaction.[6,11] Pioneering works on some bio-oil model compounds with traditional hydrodesulfurization/hydrogenation catalysts showed encouraging results.[3] Although, in addition to the requirement to keep the catalyst in sulfated form, quick deactivation due to surface oxide formation in the presence of a large amount of water was observed.[12−14] To

Received: November 3, 2022
Revised: December 21, 2022

tackle the shortcomings of sulfide catalysts, new ones were developed, among which noble and transition metal catalysts are included.[15] Transition and noble metal catalysts may exhibit superior activities, but are susceptible to coke formation.[16] In the hydrodeoxygenation of guaiacol using noble metal catalysts, adsorption of large aromatic compounds upon the catalyst surface caused significant coking-related deactivation.[17] In light of this, large-scale utilization of these materials was hindered.[11]

At milder reaction conditions, transition metals have been shown to exhibit excellent hydrogenation activity and, by extension, displayed relatively little propensity for water-accelerated deactivation.[13] Metal sites mostly promote the hydrogenation function, while catalytic HDO of bio-oil progresses through both hydrogenation and deoxygenation. There is need for a good catalyst support to promote the hydrogenation and deoxygenation reactions. Hence, the focus of recent research works has been to identify better solid-support candidates.[18,19]

A number of catalyst supports have been investigated to enhance catalyst performance.[13,20−24] Activity of a catalyst during a HDO reaction is greatly influenced by the acidity and pore structure of the support.[25−29] In comparison to metal-microporous support catalysts, metal-mesoporous support catalysts showed remarkable performances in the HDO of bio-oil. This was attributed to the improved diffusion properties and enhanced metal−support interactions.[11,30] For instance, in the HDO of guaiacol using nickel-based bifunctional catalysts, mesoporous Ni/HBeta was more selective to aromatics than microporous Ni/ZSM-5.[31] Bhoi et al.[32] reported the HDO of glycerol over Pt- and Pd-based ZSM-5 and $SiO_2$ catalysts. Therein, superior catalytic activity was observed on Pd/ZSM-5 as against $SiO_2$-supported catalysts. The HDO of anisole using natural zeolite (BEA and MOR)-supported Ni catalysts revealed that both metal and acid sites are required for the reaction. The transformation of anisole to cyclohexane was made possible by the strong Brønsted acid sites and several small Ni species over 5%Ni/BEA.[33]

Solvent compositions could affect the distributions of the catalyst and reactant in the reacting mixture and the adsorption of the reactant onto the catalyst active sites during the hydrodeoxygenation reaction. This may further affect catalytic activity and product distribution.[6] When water, octane, and decalin were compared in the HDO of guaiacol over a Ni/$TiO_2$-$ZrO_2$ catalyst, different levels of conversion and product selectivity were recorded.[23]

In the present work, the effects of support properties and solvent during the HDO reaction of anisole have been investigated. Anisole has been selected as the model compound for the catalytic test because it has a methoxy−phenyl group which is typical of lignin depolymerization fractions present in pyrolysis bio-oils derived from lignocellulosic biomass. To explore further the relationship between the reacting molecule size, acidity, and pore size of a support, as well as diffusion properties in the pores, a microporous HZSM-5 support (mic-ZSM-5, Si/Al = 16), a hierarchical ZSM-5 support (hie-ZSM-5, Si/Al = 15), and a mesoporous silica ($SiO_2$) support have been tested. Since solvent compositions could have significant effects on the extent of hydrodeoxygenation and product distribution, an aromatic compound, decahydronaphthalene (decalin), and an aliphatic hydrocarbon, *n*-decane, were tested as solvents in this study. The overall objective was to establish catalytic reaction conditions that will provide total hydrodeoxygenation of anisole and tailored selectivity toward a single liquid product.

## 2. EXPERIMENTAL SECTION

**2.1. Materials.** Anisole (99%), cyclohexane (99.8%), cyclohexene (99.5%), cyclohexanone (99%), cyclohexanol (99.5%), phenol (99%), benzene (99.5%), toluene (99.5%), methylcyclopentane (99.5%), dimethoxycyclohexane (99%), formic acid (96%), *n*-decane (98%), ammonium (II) nitrate (99%), nickel(II) nitrate hexahydrate (99.9%), and sodium hydroxide (98%) were all purchased from Sigma-Aldrich. ZSM-5 ($SiO_2/Al_2O_3$ = 30), silicon oxide catalyst support, and decahydronaphthalene (cis + trans, 98%) were purchased from Alfa Aesar. No further purification was performed on any of these chemicals.

**2.2. Preparation of Mesoporous ZSM-5 Support.** Conventional microporous ZSM-5 zeolite ($SiO_2/Al_2O_3$ = 30) in ammonium form was changed to hydrogen form via calcination for 5 h at 550 °C at a 10 °C $min^{-1}$ heating rate. The resulting mic-HZSM-5 was transformed into a mesoporous support according to the procedure reported in the literature.[34−36] That is, 5.0 g of the mic-HZSM-5 support was weighed and transferred into a glass beaker containing 150 mL of a 0.2 M sodium hydroxide solution. The mixture was placed on a magnetic stirrer, mixed, heated, and maintained at 65 °C for 1 h. The mixture was then allowed to cool and be filtered. The residue was washed repeatedly with deionized water until a filtrate with a neutral pH was obtained. The recovered sample was first dried at 80 °C for 5 h, then at 100 °C overnight. To remove alumina debris, the dried sample was treated with 200 mL of 0.2 M formic acid at 60 °C for 6 h with stirring. The resulting sample was recovered via vacuum filtration and dried. The sample was then converted to ammonium form by ion exchange three times with 500 mL of 0.5 M ammonium nitrate at 60 °C for 5 h. Finally, the treated ammonium form ZSM-5 was calcined at 550 °C for 5 h. The retrieved mesoporous support was denoted hie-ZSM-5.

**2.3. Catalyst Preparation.** Nickel was incorporated onto mic-HZSM-5, hie-HZSM-5, and the mesoporous silica support via the incipient wetness impregnation technique. Here, 5 g of support was dispersed in 20 mL of deionized water; thereafter, a solution of nickel(II) nitrate hexahydrate [$Ni(NO_3)_2{\cdot}6\ H_2O$] containing a calculated amount of nickel that is equivalent to 5 wt % loading was carefully released dropwise into a beaker holding the support slurry. The mixture was maintained at 70 °C under magnetic stirring until most of the associated liquid vaporized. Subsequently, the resulting catalyst was dried at 80 °C overnight followed by calcination at 500 °C for 3 h. Finally, these catalysts were obtained: mic-5%Ni/ZSM-5, hie-5%Ni/ZSM-5, and 5%Ni/$SiO_2$.

**2.4. Catalyst Characterization.** The crystallographic natures of the prepared samples were determined using an X-ray diffraction (XRD) Bruker D8 Advance machine. Diffraction patterns were recorded for the $2\theta$ angle range from 5° to 70° with 0.05 step increase. Nitrogen adsorption−desorption analyses were performed on Micromeritics 3-Flex analytical instrument at 77 K. The catalyst surface area was calculated based on the equation of Brunaur−Emmett−Teller (BET). Pore size distribution was determined by t-plot and Barrett−Joyner−Halenda (BJH) methods. The morphologies and chemical compositions of the catalysts were analyzed using a Hitachi TM3030 SEM-EDX machine. Acidities of the materials were determined by ammonia temperature-programmed desorption ($NH_3$-TPD) on a ChemBET apparatus equipped with a thermal conductivity detector. The sample (100 mg) was pretreated at 300 °C under flowing helium (30 mL/min) for 1 h. It was then cooled to 50 °C and adsorbed to saturation by $NH_3$/He for 30 min. Physically adsorbed $NH_3$ on the catalyst was removed by flushing the sample with helium (30 mL/min) for 1 h at the adsorption temperature. Subsequently, thermal desorption signals were recorded in the temperature range of 50−1000 °C at 10 °C/min ramp rate. $H_2$-TPR chemisorption data were collected on a Hiden Analytical CatLab. After 100 mg of the sample was pretreated in 20% $O_2$/Ar at 600 °C for 30 min and cooled to 50 °C, the $H_2$-TPR was recorded in


https://doi.org/10.1021/acs.energyfuels.2c03734
Energy Fuels XXXX, XXX, XXX−XXX

**Table 1. Reaction Factors and Their Levels**

| Factor | Level | | | | | | | | |
|---|---|---|---|---|---|---|---|---|---|
| Temperature (°C) | 150 | 150 | 150 | 200 | 200 | 200 | 250 | 250 | 250 |
| Pressure (bar) | 20 | 40 | 60 | 20 | 40 | 60 | 20 | 40 | 60 |

10% $H_2$/Ar with a heating rate of 10 °C $min^{-1}$ and a final temperature of 800 °C. Transmission electron microscopy (TEM) images were recorded using Jeol 1400 instrument. Thermogravimetric analysis was performed on a PerkinElmer TGA 8000 machine at a heating rate of 20 °C $min^{-1}$.

**2.5. Process Variables Optimization.** Various design of experiment (DOE) approaches have been reported to provide predictive knowledge of complex and multivariable processes with fewer numbers of experimental runs.[21,37,38] Here, a classical approach using JMP software was employed to analyze the contributions of temperature and pressure toward conversion and yield of products during the HDO of anisole over the mic-Ni/ZSM-5 catalyst. Temperatures of 150, 200, and 250 °C and pressures of 20, 40, and 60 bar were tested. A preliminary run guided the choice of minimum and maximum temperatures used. Virtually no reaction was seen at 120 °C at all pressures, whereas about 30% conversion was recorded at 150 °C. Conversion reached 100% at 250 and 280 °C; however, lower cyclohexane yield was generated at the higher temperature. To ensure the effect of mass transfer was eliminated during the HDO reaction of anisole over the prepared catalysts and that the reaction is kinetically controlled, another preliminary study was carried out on the effect of stirring rate on anisole conversion. An increase in the stirring speed from 800 to 1000 rpm and subsequently to 1200 rpm did not show any significant improvement in the conversion. Therefore, since the conversion plateaued at 800 rpm, it was selected for subsequent experimental runs. Table 1 presents the factors examined and their levels.

**2.6. Catalytic Activity Test and Product Analysis.** The catalytic upgrading reaction was carried out with anisole as the bio-oil model compound. Prior to the hydrodeoxygenation reaction, the catalyst was reduced ex situ in a furnace at 500 °C for 3 h under continuous flow of hydrogen (5% $H_2/N_2$) at heating rate of 5 °C $min^{-1}$. A mixture of decalin (50 mL) containing 3 wt % anisole and 100 mg of the catalyst was charged into a reactor (Parr Instruments Company, Model 4598) which was equipped with a thermocouple, a pressure gauge, a mechanical stirrer, and a controller system. The reactor was flushed three times with nitrogen then pressurized to 20 bar and heated to the desired reaction temperature (150−250 °C), during the heating-up period the stirring rate was maintained at 100 rpm. The nitrogen was thereafter replaced with 20−60 bar hydrogen. Subsequently, the reactor was mixed for 1−3 h at a stirring rate of 800 rpm. Heating-up and cooling-down periods were not considered as part of the reaction time. Liquid product was recovered from the solid catalyst by filtration.

Liquid products from the HDO reaction were analyzed using an Agilent GC (model 6890N) equipped with a flame ionization detector (FID) and a Zebron ZB-Wax capillary column (30 m × 0.25 mm × 0.25 μm). Injector and detector temperatures were set at 250 and 270 °C, respectively. While the carrier gas was helium, the liquid injection volume was 1 μm, and a split ratio of 280:1 was used. The oven was programmed as follows: initial temperature of 35 °C was held for 2 min, increasing to 200 °C at a ramp rate of 20 °C $min^{-1}$, then to 220 °C at a ramp rate of 35 °C $min^{-1}$ and held for 2.5 min. Before sample analysis, the GC was calibrated with the chemical standard of the expected products (methyl-cyclohexane, cyclohexane, cyclohexene, cyclohexanol, cyclohexanone, anisole, methoxycyclohexane, benzene, toluene, and phenol) for identification and quantification. To evaluate the extent of anisole conversion ($X_{anisole}$), yield of product ($Y_i$), selectivity ($S_i$), degree of hydrodeoxygenation (selectivity to products with no oxygen, HDO %), degree of hydrodearomatization (selectivity to products with no aromatics, HDA %), and carbon balance, the following expressions were used.

$$X_{anisole}\,(\%) = \frac{\text{moles of anisole consumed}}{\text{moles of anisole in the feed}} \times 100 \quad (1)$$

Since 1 mol of anisole will only produce 1 mol of cyclohexane or 1 mol of toluene, then

$$Y_i\,(\%) = \frac{\text{moles of product } i \text{ formed}}{\text{moles of anisole in the feed}} \times 100 \quad (2)$$

$$S_i\,(\%) = \frac{\text{moles of product } i \text{ formed}}{\text{moles of anisole consumed}} \times 100 \quad (3)$$

$$\text{HDO}\,(\%) = \left(1 - \frac{\Sigma(\text{moles of product } i \times \text{number of oxygen atoms in } i)}{\text{moles of anisole in the feed} \times \text{anisole conversion}}\right) \times 100 \quad (4)$$

$$\text{HDA}\,(\%) = \left(1 - \frac{\Sigma(\text{moles of product } i \times \text{number of aromatic rings in } i)}{\text{moles of anisole in the feed} \times \text{anisole conversion}}\right) \times 100 \quad (5)$$

$$\text{Carbon balance}\,(\%) = \frac{C_{\text{total-products}}}{C_{\text{total-anisole}}} \times 100 \quad (6)$$

where $C_{\text{total-products}}$ is the number of total carbon atoms of detectable products in the reaction solution, and $C_{\text{total-products}}$ is the number of total carbon atoms of anisole in the feed solution.

## 3. RESULTS AND DISCUSSION

**3.1. Catalyst Characterization.** The XRD patterns of the parent zeolite (mic-ZSM-5), NaOH-treated zeolite (hie-ZSM-5), their Ni-based catalysts, $SiO_2$, and Ni/$SiO_2$ are presented in Figure 1. No noticeable destruction of the zeolite framework

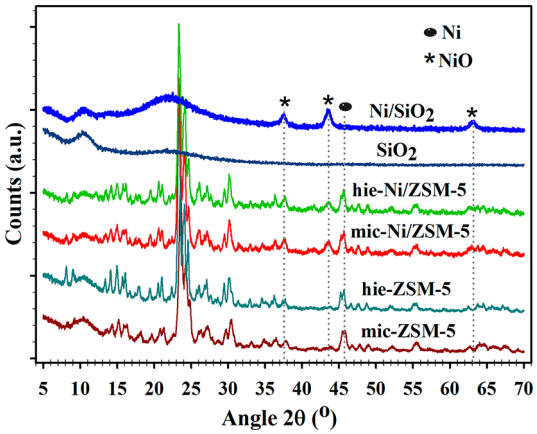


**Figure 1.** XRD patterns of ZMS-5 and $SiO_2$ supports and their 5 wt % Ni-based catalysts.

was observed due to the NaOH treatment; hie-ZSM-5 retained all the characteristic diffraction peaks observed in the parent material. However, reductions in the peaks' intensities in the treated material compared to the parent zeolite were noticed. This was due to the extraction of framework silicon by NaOH;[36] hence, a decrease in crystallinity from 100% to 89.9% was noted as shown in Table 2. Following nickel impregnation,


https://doi.org/10.1021/acs.energyfuels.2c03734
Energy Fuels XXXX, XXX, XXX−XXX

**Table 2. Percentage Crystallinity and Crystallites Sizes Calculated from XRD Data**

| Sample | Crystallinity (%) | Average crystallite size (nm) | NiO crystallite size (nm) |
|---|---|---|---|
| mic-ZSM-5 | 100 ± 0.00 | 27.05 ± 0.21 | – |
| hie-ZSM-5 | 90.05 ± 0.21 | 26.80 ± 0.42 | – |
| mic-Ni/ZSM-5 | 87.55 ± 0.21 | 30.70 ± 0.71 | 12.60 ± 0.85 |
| hie-Ni/ZSM-5 | 84.40 ± 0.85 | 29.05 ± 0.35 | 11.85 ± 0.78 |
| $Ni/SiO_2$ | – | – | 14.75 ± 0.21 |

new diffraction peaks at $2\theta$ = 37.6°, 43.7°, and 46.7° were observed for both mic-Ni/ZSM-5 and hie-Ni/ZSM-5 catalysts, which were ascribed, respectively, to NiO (111), NiO (200), and Ni (111) planes.[14,39] The peak at 43.7° was the typical diffraction peak of NiO crystals.[40] Similarly, successful deposition of nickel on the $SiO_2$ support could be confirmed from the XRD spectra with the identification of peaks at $2\theta$ = 37.5°, 43.7°, and 63.2 corresponding, respectively, to NiO planes (111), (200), and (220).[41,42] A broad peak was observed between $2\theta$ = 20°−30°, which indicates the amorphous nature of the silica support.

Average crystallite sizes of the materials were estimated from the XRD data using a line broadening technique (Scherrer equation). mic-ZSM-5 and hie-ZSM-5 have crystallite sizes of 27.05 ± 0.21 and 26.80 ± 0.42 nm, respectively. These crystallite sizes increased to 30.70 ± 0.71 and 29.05 ± 0.5 nm after nickel was impregnated onto the respective supports. Crystallite sizes of NiO were determined to be 12.6 ± 0.85, 11.85 ± 0.78, and 14.75 ± 0.21 nm for mic-Ni/ZSM-5, hie-Ni/ZSM-5, and $Ni/SiO_2$ catalysts, respectively. The effect of crystallite size on catalytic activity has been reported in the literature.[31,43] Fu et al.[44] noticed this effect only when the nickel particle size was greater than 10 nm during the hydrogenation of glucose over a nickel-supported carbon catalyst. A particle size of 17 nm exhibited superior catalytic activity, with higher glucose conversion and product yield compared to a catalyst with a 22 nm nickel particle size. Similarly, during the methanation of $CO_2$, the highest catalytic activity and $CH_4$ selectivity were recorded on a Ni-supported catalyst with a particle size of 19 nm, compared with 32 and 46 nm.[45]

Figure 2 presents the nitrogen adsorption−desorption isotherms and pore structures of both the supports and their corresponding nickel catalysts. The BJH method was used for the determination of pore size distribution. The BET surface area and total pore volume calculated from the measurements as well as the Si/Al ratio determined using EDX are summarized in Table 3. An increase in $N_2$ adsorption between $p/p_0$ = 0.4−0.8 on the mic-ZSM-5 support indicates the presence of some mesopores in the material. In addition, the isotherm is more like a Type I isotherm which is characterized with high fractions of fine micropores and low fractions of mesopores, based on IUPAC classification.[36] There was a noticeable increase in the quantity of adsorbed $N_2$ and a shift from Type I to Type II isotherms after mic-ZSM-5 was treated with 0.2 M NaOH to produce the hie-ZSM-5 support. The hie-ZSM-5 support shows a hysteresis loop (Type H4) at higher relative pressure, indicating the presence of mesopores.[31] $SiO_2$ and $Ni/SiO_2$ exhibit marked uptake of the Type IV isotherm with the H2 type hysteresis loop at $p/p_0 > 0.75$, showing mesoporous characteristics due to a capillary condensation process.[43]

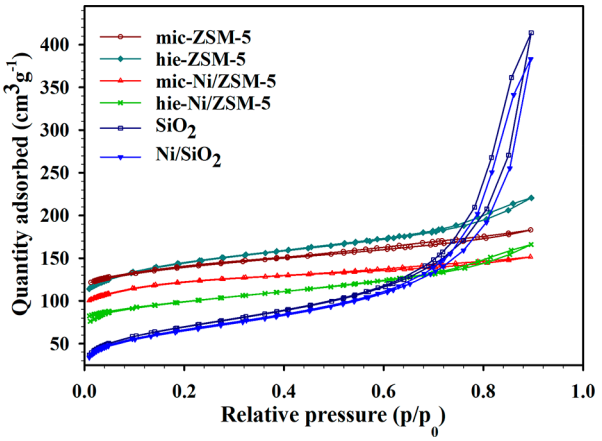


**Figure 2.** Nitrogen adsorption−desorption isotherms of ZSM-5 and silica supports and their 5 wt % Ni-based catalysts at 77 K.

Following the NaOH treatment, the surface area of ZSM-5 increased from 434 to 459 $m^2\ g^{-1}$ in addition to the formation of more mesopores. Compared to the conventional ZSM-5, a hierarchical ZSM-5 is characterized by enhanced surface area.[34,44−46] Loading of Ni caused an evident decrease in the surface area and total volume for all the supports, suggesting that nickel particles have been effectively deposited.[44] The observed decreases in pore volume and surface area after nickel incorporation are attributed to partial blockage of pores due to the metal loading.[47] As established from Table 3, there were decreases of 0.049, 0.085, and 0.048 $m^3g^{-1}$, respectively, in the total pore volume after 5 wt % nickel impregnations on the mic-ZSM-5, hie-ZSM-5, and $SiO_2$ supports. For all the supports, metal loading caused a greater decrease in mesopore volumes than micropore volumes. The decreases were 57.1%, 55.3%, and 97.9% for mic-ZSM-5, hie-ZSM-5, and $SiO_2$, respectively. A slight decrease in the Si/Al ratio from 16 to 15, also shown in Table 3, is caused by the extraction of framework silica due to the NaOH treatment. There were reports on a decrease in the Si/Al ratio when microporous ZSM-5 was treated with 0.1, 0.2, 0.3, and 0.4 M of NaOH.[36,48] However, pioneering work by Rac et al.[34] reported improved mesoporous properties and demonstrated nearly full preservation of both the Si/Al ratio and the acid site strength when ZSM-5 ($SiO_3/Al_2O_3$ = 50) was treated with 0.2 M NaOH.

The morphologies of the supports were investigated using SEM. Both mic-ZSM-5 and hie-ZSM-5 showed agglomerates of very fine particles with sizes ranging between 0.5−2 $\mu$m as shown in Figure S1. However, hie-ZSM-5 exhibited less agglomeration compared to mic-ZSM-5. A sponge-like assembly of small and nonuniform particles with an average size of 5.8 $\mu$m was observed for $SiO_2$. Figure 3(a, c, e) presents the SEM images of the catalysts on addition of 5 wt % nickel. These show signs of good metal dispersion and formation of heterostructures. To complement the SEM figures, TEM images were captured to display finer detail and are shown in Figure 3(b, d, f). It is clear that there is a high degree of metal dispersion, particularly in ZSM-5. The nickel particles there are smaller than those on the $Ni/SiO_2$ catalyst and therefore difficult to distinguish. On the other hand, the $Ni/SiO_2$ catalyst shows larger nickel particle size with an average length of 15 nm. This finding reflects the XRD result in which the diffraction peaks for NiO are more obvious in the $Ni/SiO_2$ catalyst compared to the Ni/ZSM-5 catalysts.


https://doi.org/10.1021/acs.energyfuels.2c03734
Energy Fuels XXXX, XXX, XXX−XXX

**Table 3. Textural Properties of ZSM-5 and $SiO_2$ Supports and Prepared Ni Catalysts**

| Sample | Si/Al ratio[a] | $S_{BET}$[b] ($m^2g^{-1}$) | $S_{micro}$[c] ($m^2g^{-1}$) | $S_{meso}$(%) | $V_{total}$[d] ($m^3g^{-1}$) | $V_{micro}$[e] ($m^3g^{-1}$) | $V_{meso}$[f] ($m^3g^{-1}$) | Average pore width[g](nm) |
|---|---|---|---|---|---|---|---|---|
| mic-ZSM-5 | 16 | 434 | 276 | 36 | 0.284 | 0.147 | 0.137 | 3.98 |
| hie-ZSM-5 | 15 | 459 | 238 | 48 | 0.342 | 0.126 | 0.216 | 4.63 |
| hie-Ni/ZSM-5 | 15 | 316 | 166 | 48 | 0.257 | 0.088 | 0.169 | 4.97 |
| mic-Ni/ZSM-5 | 16 | 378 | 236 | 38 | 0.235 | 0.126 | 0.109 | 3.68 |
| $SiO_2$ | – | 248 | 10 | 96 | 0.642 | 0.004 | 0.638 | 10.43 |
| $Ni/SiO_2$ | – | 232 | 9 | 96 | 0.594 | 0.003 | 0.591 | 10.31 |

[a]EDX. [b]From $N_2$ adsorption measurement. [c]From $N_2$ adsorption measurement (t-plot). [d]From $N_2$ adsorption measurement at $p/p_0$ = 0.8942. [e]From $N_2$ adsorption measurement (t-plot). [f]Difference between d and e ($V_{total} - V_{micro}$). [g]From BJH method.

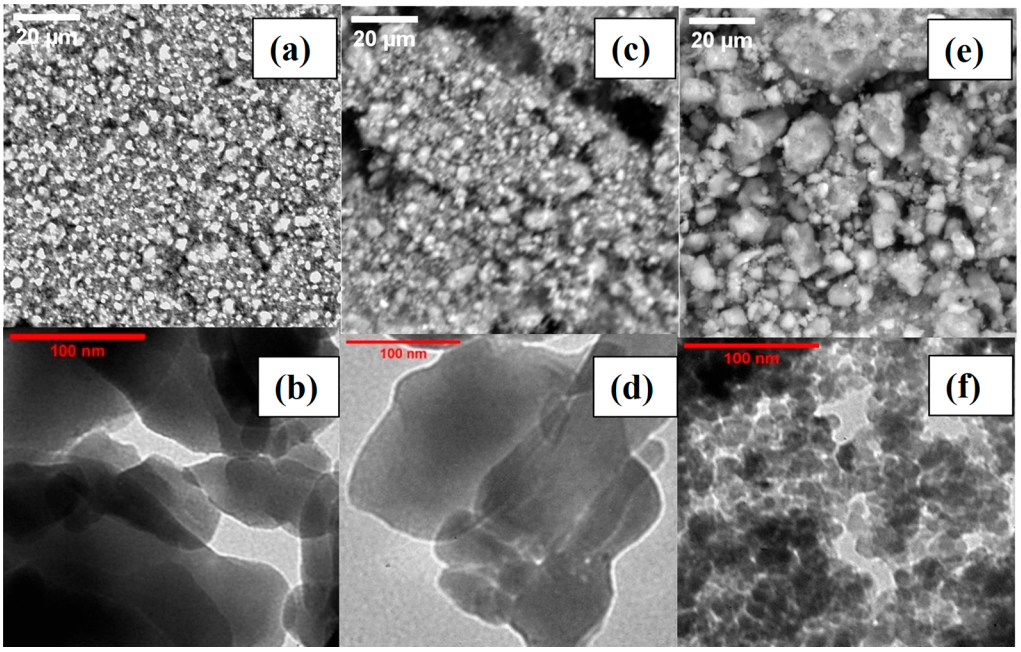


**Figure 3.** SEM and TEM images of mic-Ni/ZSM-5 (a, b), hie-Ni/ZSM-5 (c, d), and $Ni/SiO_2$ (e, f) catalysts.

**Table 4. EDX Elemental Mapping Results of ZSM-5 Supports and Ni-Based Catalysts**

| Element (%) | mic-ZSM-5 | hie-ZSM-5 | mic-Ni/ZSM-5 | hie-ZSM-5 | $Ni/SiO_2$ |
|---|---|---|---|---|---|
| O | 53.77 | 52.29 | 50.52 | 50.43 | 50.24 |
| Si | 35.46 | 35.72 | 28.68 | 28.27 | 35.23 |
| Al | 2.21 | 2.3 | 1.81 | 1.75 | 0.00 |
| Ni | 0.00 | 0.00 | 4.26 | 4.60 | 5.44 |
| Others | 8.56 | 9.68 | 14.78 | 13.70 | 9.09 |
| Total (%) | 100 | 100 | 100 | 100 | 100 |

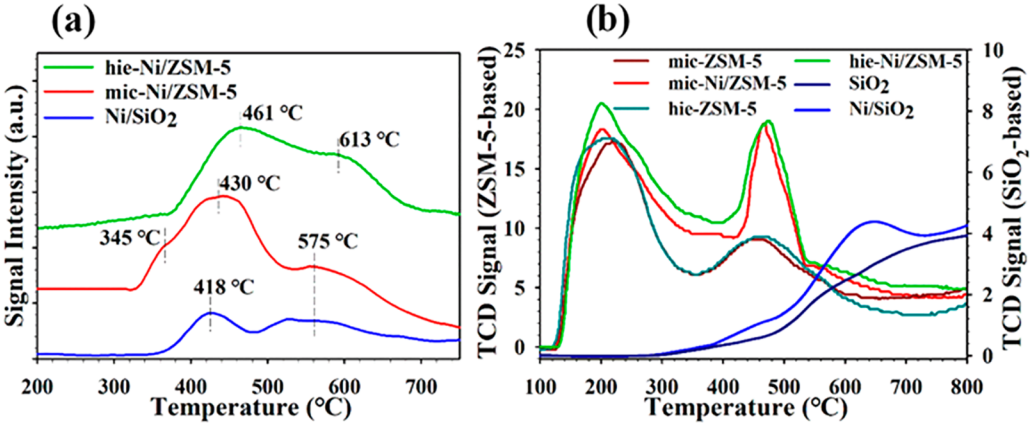


**Figure 4.** (a) $H_2$-TPR and (b) $NH_3$-TPD profiles of catalysts.


https://doi.org/10.1021/acs.energyfuels.2c03734
Energy Fuels XXXX, XXX, XXX−XXX

EDX elemental mapping was used to visualize and quantify the distribution of elements on the catalysts. Table 4 presents the percentage compositions of Si, Al, O, and Ni in the samples. The targeted metal loading of 5% was approximately achieved (±0.51 mean deviation). Expectedly, nickel was not detected in the supports.

The presence of Ni species on the three catalysts was further investigated using $H_2$-TPR analysis, shown in Figure 4(a). $H_2$-TPR provides information about the metal reduction temperature, strength of the metal−support interaction, and reducibility of the metal within a support.[49] Two reduction peaks at 418 and 575 °C were found for the $Ni/SiO_2$ catalyst indicating the presence of two different types of NiO species.[39] While three reduction peaks centered at around 345, 430, and 575 °C were recorded for the mic-Ni/ZSM-5 catalyst, only two peaks were observed for the hie-Ni/ZSM-5 catalyst. However, a shift in the positions of peaks from 430 and 575 °C on mic-Ni/ZSM-5 to 461 and 613 °C on hie-Ni/ZSM-5 were noticed. Lower temperature peaks were attributed to a weak interaction between nickel oxide and the surfaces of the supports. A reduction temperature below 400 °C shows the occurrence of small extent of ion exchange and that NiO is on the exterior surface of the support. A peak at higher temperature implies a strong metal−support interaction. Similarly, high temperature is required when the NiO species are beside the support surface or the NiO crystallites are larger.[14,44,50] It is significant to note that mic-Ni/ZSM-5 shows a minor peak below 400 °C indicating some NiO particles are dispersed on the external surface of the support. Compared with hie-Ni/ZSM-5 and $Ni/SiO_2$ catalysts, the hydrogen consumption peaks were above 400 °C indicating good dispersion of NiO within the pores of the supports and/or larger NiO particles on the exterior surface of the support. However, with the decrease in total pore volume observed after nickel impregnation from the BET results, it could be concluded that a reasonable amount of nickel was properly dispersed within the pores of hie-ZSM-5. The decreases in total pore volumes after nickel impregnation on the supports, as determined from Table 3, were 0.085, 0.049, and 0.048 $m^3g^{-1}$ for hie-ZSM5, mic-ZSM-5, and $SiO_2$, respectively. Therefore, the strengths of metal−support interactions for the three catalysts decrease in the following order: hie-Ni/ZSM-5 > mic-Ni/ZSM-5 > $Ni/SiO_2$.

Figure 4(b) presents the measure of acidity of the catalysts performed by temperature-programmed desorption (TPD) using ammonia as the probe molecule. The ZSM-5 sample exhibited dual desorption peaks between 130−350 °C and 350−580 °C which agrees with the acidity data for MFI materials reported in the literature.[51] The $SiO_2$-based sample displayed a broad range of peaks between 300 and 750 °C. The high-temperature and low-temperature peaks were, respectively, attributed to the $NH_3$-desorption from the strong and the weak acid sites centers. Peak temperature and area are linked to the acid strength and acid sites concentration.[14,52,53] It is obvious from the result presented in Table 5 that incorporation of nickel onto the support generated a new desorption peak for $SiO_2$ and broadened the low-temperature peaks for ZSM-5, as well as narrowing and reducing the area of the high-temperature peaks. Formation of new peaks were reported when transition metals such as nickel were introduced onto a catalyst support.[14] For the quantitative evaluation of the acid sites, the $NH_3$-TPD profiles were deconvoluted into three distinct peaks corresponding to weak, medium, and strong acid sites using the Gaussian fitting method, shown in Figure S2.

**Table 5. Acidic Property of Supports and Corresponding 5 wt % Ni-Based Catalysts**

| | | Acid site concentration (%) | | | Peak temperature[a] (°C) | | |
|---|---|---|---|---|---|---|---|
| Sample | Total peak area (a.u.)[2] | Weak | Medium | Strong | $T_{pw}$ | $T_{pm}$ | $T_{ps}$ |
| mic-ZSM-5 | 3292 | 35 | 13 | 52 | 227 | 286 | 447 |
| hie-ZSM-5 | 3346 | 33 | 20 | 47 | 221 | 282 | 451 |
| mic-Ni/ZSM-5 | 3445 | 54 | 22 | 24 | 241 | 362 | 473 |
| hie-Ni/ZSM-5 | 4539 | 42 | 35 | 23 | 240 | 353 | 473 |
| $SiO_2$ | 788 | 0 | 0 | 100 | – | – | 682 |
| $Ni/SiO_2$ | 829 | 0 | 14 | 86 | – | 456 | 634 |

[a] $T_{pw}$, $T_{pm}$, $T_{ps}$ = Peak temperatures for weak, medium, and strong acid sites.

Table 5 also presents a summary of the acid site concentration and distribution from the deconvoluted $NH_3$-TPD curves. Compared with the parent zeolite (mic-ZSM-5), there was an evident increase in the acid site concentration in hie-ZSM-5. In addition, hie-ZSM-5 possessed a lower amount of strong acid sites compared to mic-ZSM-5 suggesting that the NaOH treatment reduces the acid properties of the support. With a low degree of crystallinity and more mesopores, as respectively quantified by the XRD and BET results, hie-ZSM-5 is expected to possess less coordinating aluminum in the framework, leading to a lower strong acid site concentration. This finding is in agreement with the previous reports that microporous zeolites usually have higher strong acid site concentrations than their mesoporous counterparts.[14] Impregnating the parent and the treated ZSM-5 with nickel increased, significantly, the weak acid site concentration and, slightly, the medium acid site concentration, while the strong acid site concentration decreased. According to Tu et al.,[14] nickel-based catalysts normally show improved weak acid site concentration. A similar trend was reported by a number of researchers.[1,44,54] Notably, the total acidity of the $Ni/SiO_2$ catalyst is more than four times larger than the total acidity of the Ni/ZSM-5 catalyst. The deconvoluted profile of $Ni/SiO_2$ shows a peak centered at 456 °C which might be linked to medium acid sites, owing to the presence of unreduced nickel species in the form of Ni-Si.[55,56]

**3.2. Activity Test.** HDO of anisole involves a number of parallel/series transformation steps. Previous works have reported several reaction sequences.[44,49,57,58] Depending on the type of catalyst, degree of deoxygenation, and extent of hydrogenation, some of the possible products and intermediates of the reaction are cyclohexane, methylcyclopentane, phenol, benzene, toluene, cyclohexene, cyclohexanone, cyclohexanol, ethers, and transalkylates. In addition, light ends such as methane, ethylene, and trace amounts of CO may be generated. Figure 5 presents time-dependent conversion, yield, and selectivity profiles of products during the HDO of anisole. Prior to the reaction, the catalysts were reduced ex situ in a furnace at 500 °C for 3 h at a heating rate of 5 °C $min^{-1}$ under a continuous flow of 5% $H_2/N_2$. Conversions were 100%, 82.6%, and 48.9%, respectively, over hie-Ni/ZSM-5, mic-Ni/ZSM-5, and $Ni/SiO_2$ catalysts within 2 h. The highest conversion on the NaOH desilicated catalyst (hie-Ni/ZSM-5) was attributed to the enhanced catalytic activity, as the


https://doi.org/10.1021/acs.energyfuels.2c03734
Energy Fuels XXXX, XXX, XXX−XXX

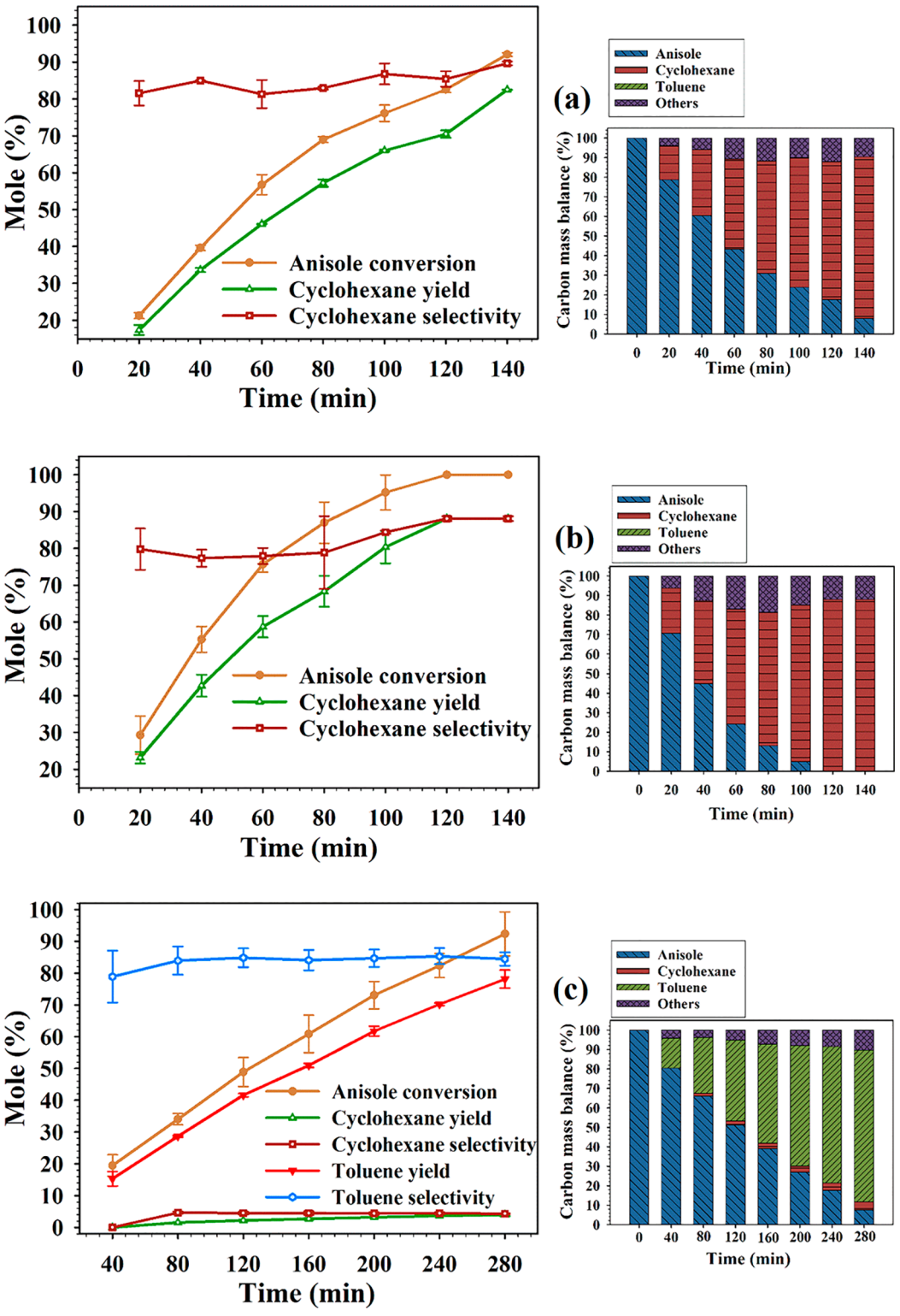


**Figure 5.** Time-dependent anisole conversion, yield, and selectivity of liquid products and carbon mass balance at 200 °C, 60 bar $H_2$, 48.65 mL of decalin, 1.35 mL of anisole, 100 mg of catalyst: (a) mic-Ni/ZSM-5, (b) hie-Ni/ZSM-5, and (c) $Ni/SiO_2$.

reactant has access to more active sites on the catalyst. In a related work, higher conversion and yield of the product were recorded after mesopores were introduced to a conventional HZSM-5 via desilication.[31] This is in agreement with the XRD, BET, and $NH_3$-TPD results which revealed good preservation of the ZSM-5 structure after NaOH treatment, high surface area and pore volume for metal dispersion, and relatively high acid site concentration. Lowest conversion was recorded on $Ni/SiO_2$, suggesting low catalytic activity. This can be related to the nature of the $SiO_2$ support which is a function of the types and concentrations of acid sites available for the reaction. However, conversion eventually reached 92.4% when the reaction was allowed to proceed for 280 min.


https://doi.org/10.1021/acs.energyfuels.2c03734
Energy Fuels XXXX, XXX, XXX−XXX

The liquid products obtained during the reaction were cyclohexane and toluene. The elemental carbon balance, shown in Figure 5, was carried out to determine the material balance within the reactor and quantify the carbon lost. The total lost, referred to as "others", is the amount of carbon in the unquantified gaseous products and possibly in liquid products below the detection limit of the GC instrument. Sankaranarayanan et al.[44] observed the formation of methane and trace quantities of CO, ethylene, and some isomers of propyl and butyl during the HDO of anisole over supported Ni and Co catalysts. In this work, the three catalysts, mic-Ni/ZSM-5, hie-Ni/ZSM-5, and Ni/$SiO_2$, achieved cyclohexane yields of 70.5%, 88.1%, and 2.2%, while the yields of other products were 12.0%, 11.9%, and 5.1%, respectively, in 2 h at 200 °C. It could be noticed that the amount of cyclohexane generated on the hie-Ni/ZSM-5 catalyst differed markedly compared with the amount of cyclohexane obtained from the mic-Ni/ZSM-5 and Ni/$SiO_2$ catalysts. This might be explained by the improved properties of the hie-ZSM-5 support which allowed reactants more access to the active sites and products to desorb easily from the catalyst surface after formation. The Ni/$SiO_2$ catalyst was 84.9% selective to toluene. Despite the high concentrations of acid sites on mic-ZSM-5 supports, a preliminary experiment showed anisole conversion of only 2% without any yield of liquid product, and a similar trend was reported.[14] Interestingly in this work, after nickel impregnation on a $SiO_2$ support, which has a low acid site concentration compared to a ZSM-5 support, a reasonable conversion as well as yield of the liquid product were obtained. This clearly demonstrated that a synergy between the acid site and active metal is crucial for the reaction. The Ni/$SiO_2$ catalyst, which has larger pores, was more selective to toluene than cyclohexane. A possible reason could be the absence of micropores that might retain the reactant or intermediates within the system for further reaction, such as demethylation and/or hydrodearomatization.

Several reaction pathways during anisole HDO were reported in literature. Tu et al.[14] proposed that anisole transformations over Ni-$Al_2O_3$ and Ni/ZSM-5 catalysts proceed via saturation of aromatic rings, rapid demethylations of methoxy-cyclohexane to cyclohexanone, and, subsequently, dehydration, of cyclohexanone to cyclohexane. This is referred to as the hydrogenation−dehydration route. Anisole HDO on zeolite Y-supported Pb, Ni, and Ru catalysts was shown to progress by the same route.[49] Another transformation route is direct deoxygenation.[44,58,59] An example of the latter is the HDO reaction of anisole over the Co/SBA-15 catalyst which was achieved by breaking down the methoxy−phenyl bond to form benzene. Thereafter, the benzene is hydrogenated to cyclohexane. Based on the product distribution observed from the mic-Ni/ZSM-5, hie-Ni/ZSM-5, and Ni/$SiO_2$ catalysts, a simple reaction scheme was proposed and is presented in Figure 6. Selectivity to cyclohexane was 88.1% and 89.6% on hie-Ni/ZSM-5 and mic-Ni/ZSM-5, respectively, at the end of the reaction. Of particular interest is that no intermediate product was seen, as samples were withdrawn from the reactor and analyzed at regular intervals of 20 min. It is hypothesized that the cleavage of methoxy group and hydrogenation of benzene to cyclohexane occurs very fast via the direct deoxygenation−hydrogenation pathway. On the other hand, high selectivity toward toluene on the Ni/$SiO_2$ catalyst could be interpreted as follows: anisole adsorbs onto the acidic sites of the catalyst which prompt a nucleophilic attack between the

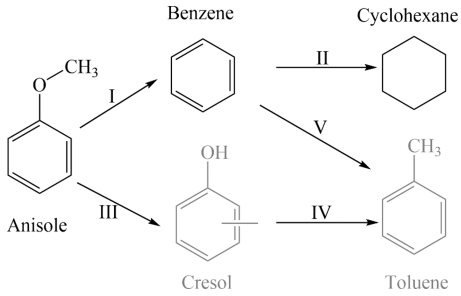


**Figure 6.** Proposed reaction scheme in anisole transformation over 5 wt % Ni/ZSM-5 and 5 wt % Ni/$SiO_2$ catalysts: (I) demethoxylation, (II) hydrogenation, (III) isomerization, (IV) direct deoxygenation, and (V) alkylation.

R−O bond forming a carbenium ion. The cleaved methyl carbenium ion is then transferred onto the aromatic ring to form cresol. Afterward, the cresol undergoes direct deoxygenation to produce toluene.

The extents of hydrodeoxygenation (HDO %) and hydrodearomatization (HDA %) were calculated based on eqs 4 and 5 (Figure S3). Since no products containing oxygen atoms or aromatic rings were visible over the hie-Ni/ZSM-5 and mic-Ni/ZSM-5 catalysts, it could be concluded there was complete hydrodeoxygenation and hydrodearomatization of the transformed reactant. However, the Ni/$SiO_2$ catalyst showed a very low hydrodearomatization capacity of 15.4%, as 84.6% of the products contained aromatic rings, confirming the need for the appropriate combination of active metals and supports for effective bio-oil upgrading.

The effects of temperature, pressure, and solvent on anisole conversion and product distribution were investigated. Figure 7(a) presents results for the HDO reaction over the temperature range between 150 and 250 °C. Anisole conversion increases with temperature, from 29.5% to 92.1% and 100% at 150, 200, and 250 °C, respectively, over mic-Ni/ZSM-5. In addition to the large increase in conversion when the reaction temperature increased from 150 to 200 °C, an increase in cyclohexane yield was also seen, going from 27.2% to 82.5% with selectivity of 92.5% at 150 °C and 89.6% at 200 °C. However, yields of other products increased from 2.2% at 150 °C to 9.6% and 15.0% at 200 and 250 °C. Contrary to this, Tu et al.[60] reported variations in selectivity during the HDO of anisole using the hierarchical Ni-zeolite catalyst. Therein, as the reaction temperature increased from 100 to 200 °C, conversion increased from 4.6% to 100%. The selectivity at the lower temperature was 86.5% to methoxy-cyclohexane and 97.0% to cyclohexane at 200 °C. The most notable points in this work are that there was total deoxygenation of the reactant and 89.6% selectivity to cyclohexane over the mic-Ni/ZSM-5 catalyst. Since cyclohexane was the only liquid product detected, further purification of the product might not be required after separating from the solid catalyst.

Figure 7(b) shows the effect of hydrogen pressure on anisole conversion. This was investigated at a fixed temperature of 200 °C and pressures of 20, 40, and 60 bar. A strong influence of hydrogen pressure could be clearly seen in the conversion of anisole and yield of products. A proportional relationship was evident between the pressure, anisole conversion, and product yield. As the pressure increased from 20 to 40 and 60 bar, the conversion increased from 54.4% to 70.4% and 92.1%, while the cyclohexane yield increased from 46.5% to 61.0% and 82.5%, respectively. Although, at high pressure, it is widely


https://doi.org/10.1021/acs.energyfuels.2c03734
Energy Fuels XXXX, XXX, XXX−XXX

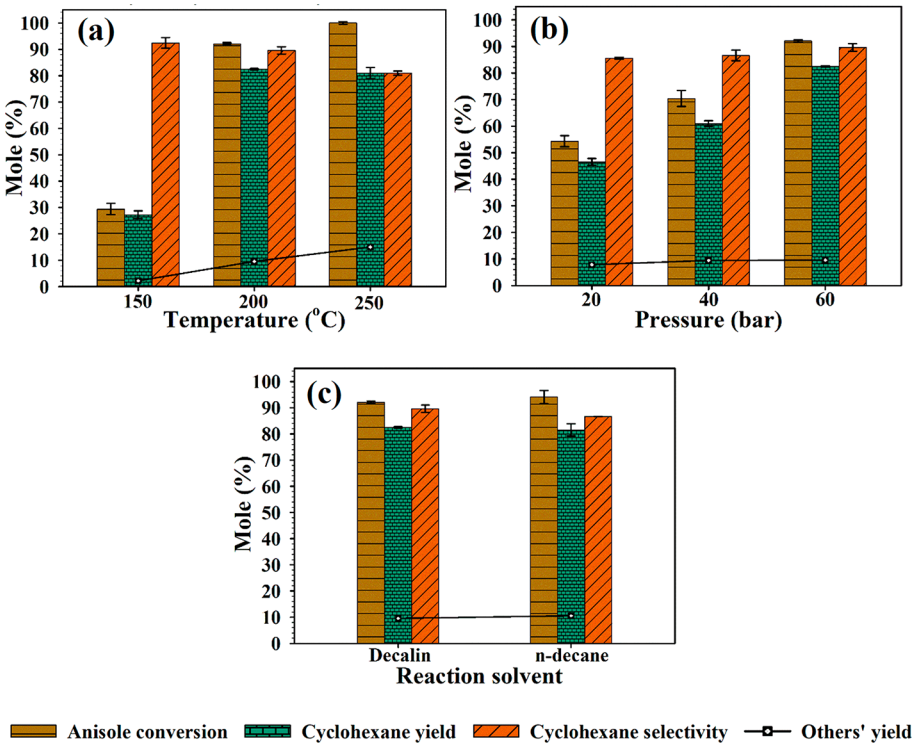


**Figure 7.** Effects of (a) temperature at 60 bar $H_2$, (b) pressure at 200 °C, and (c) solvent at 200 °C, 60 bar $H_2$ on anisole conversion, and product distribution over a mic-Ni/ZSM-5:50 mL mixture of 3.0 wt % anisole and 100 mg of catalyst.

**Table 6. Effect of Temperature on Product Distribution during HDO of Anisole**[a]

| | | | Selectivity (mole %) | | |
|---|---|---|---|---|---|
| Sample | Temperature (°C) | Conversion (mole %) | Cyclohexane | Toluene | Others |
| mic-Ni/ZSM-5 | 180 | 71.33 | 93.83 | 0.0 | 6.17 |
| | 200 | 92.05 | 89.62 | 0.0 | 10.38 |
| | 220 | 100 | 82.62 | 0.0 | 17.38 |
| | 240 | 100 | 79.31 | 0.0 | 20.70 |
| hie-Ni/ZSM-5 | 180 | 73.61 | 95.61 | 0.0 | 4.39 |
| | 200 | 100 | 88.09 | 0.0 | 11.91 |
| | 220 | 100 | 87.20 | 0.0 | 12.80 |
| | 240 | 100 | 82.22 | 0.0 | 17.78 |
| $Ni/SiO_2$ | 180 | 32.66 | 4.50 | 92.62 | 2.88 |
| | 200 | 92.38 | 4.32 | 84.58 | 11.10 |
| | 220 | 100 | 7.27 | 75.84 | 16.88 |
| | 240 | 100 | 13.04 | 72.40 | 14.57 |

[a]Conditions: 60 bar $H_2$, 48.65 mL of decalin, 1.35 mL of anisole, 100 mg of catalyst.

known that aromatic ring hydrogenation is favored over direct deoxygenation.[61] Herein, no liquid product containing an oxygen atom was detected at any point during the reaction within the range of pressure investigated. Strong dependency of anisole conversion on hydrogen pressure was also reported by Ghampson et al.,[58] who demonstrates that the demethoxylation (direct deoxygenation) pathway is most significantly influenced by changing hydrogen pressure. This may also support the anisole transformation route over mic-Ni/ZSM-5 proposed in this work.

The effect of solvent composition on the overall catalytic performance of mic-Ni/ZSM-5 was further evaluated. The reaction was performed at a temperature of 200 °C and 60 bar hydrogen for 140 min, with results shown in Figure 7(c). Anisole conversion and cyclohexane selectivity were 92.1% and 89.6%, respectively, in decalin while 94.1% conversion and 86.7% selectivity were seen in the *n*-decane environment. Although the two solvents used are different in that decalin is a bicyclic hydrocarbon consisting of two fused cyclohexane rings, whereas *n*-decane is a straight chain hydrocarbon (alkane hydrocarbon), the overall catalytic activity is virtually the same. In addition, there was complete hydrodearomatization of the products in both solvents. In contrast to what was reported here, in the literature, there were changes in conversion and product yield during the hydrodeoxygenation of guaiacol in water, octane, and decalin over the $Ni/TiO_2$-$ZrO_2$ catalyst at 300 °C and 40 bar hydrogen pressure. Conversion and


https://doi.org/10.1021/acs.energyfuels.2c03734
Energy Fuels XXXX, XXX, XXX−XXX

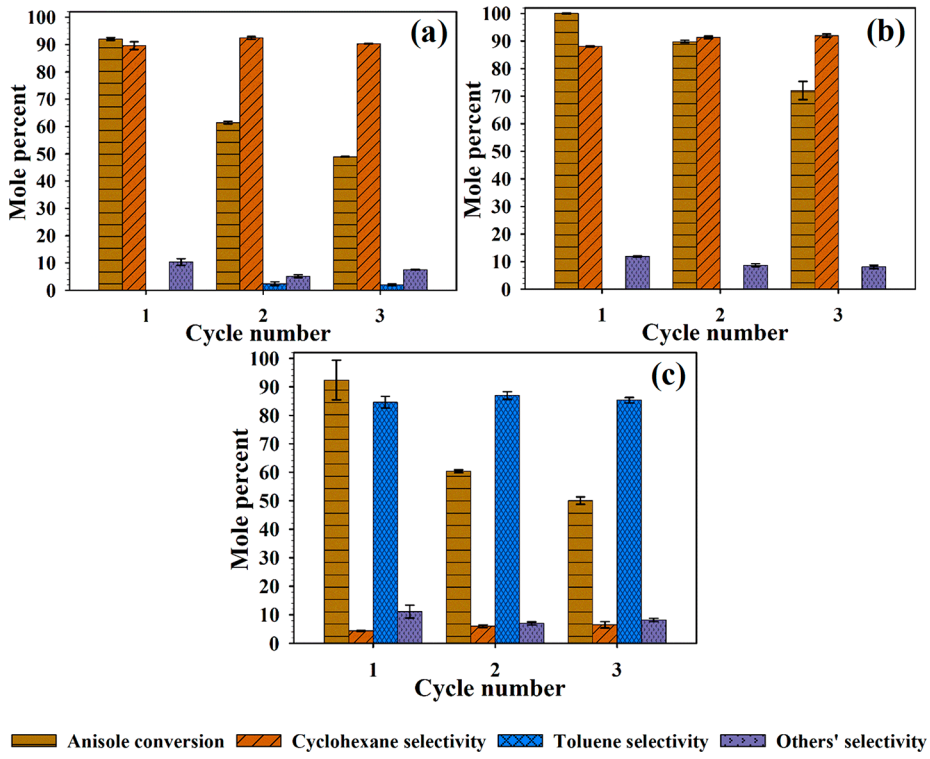


**Figure 8.** Catalysts reusability test via conversion and selectivity after each of three cycles at 200 °C, 60 bar $H_2$, 48.65 mL of decalin, 1.35 mL of anisole, 100 mg of catalyst: (a) mic-Ni/ZSM-5, (b) hie-Ni/ZSM-5, and (c) $Ni/SiO_2$.

cyclohexane selectivity were 35% and 20% in water, 60% and 30% in octane, and 100% and 89% in decalin, respectively.[23]

The effects of temperature on product distribution during anisole HDO over the mic-Ni/ZSM-5, hie-Ni/ZSM-5, and $Ni/SiO_2$ catalysts are shown in Table 6. It can be seen that an increase in temperature from 180 to 240 °C improved the overall catalytic activity by changing the conversion from 71.3% to 100% and from 73.6% to 100% on mic-Ni/ZSM-5 and hie-Ni/ZSM-5, respectively. It is evident that cyclohexane selectivity decreased from 95.6% to 82.2% on hie-Ni/ZSM-5 and from 93.8% to 79.3% over the mic-Ni/ZSM-5 catalysts as the temperature increased from 180 to 240 °C. Although, selectivity to other products increased with increasing reaction temperature in both cases. Anisole conversion increased from 32.7% at 180 °C to 100% at 240 °C over the $Ni/SiO_2$ catalyst. Unlike the mic-Ni/ZSM-5 and hie-Ni/ZSM-5 catalysts, the $Ni/SiO_2$ catalyst was 92.6% selective to toluene at 40 °C. However, increasing the reaction temperature to 240 °C reduced the selectivity to 72.4%. In addition, there was an increase in cyclohexane selectivity from 4.5% at 180 °C to 13.0% at 240 °C.

A catalyst reusability study was carried out on the mic-Ni/ZSM-5, hie-Ni/ZSM-5, and the $Ni/SiO_2$ catalysts for three reaction cycles, and the results are shown in Figure 8. As reported in the literature, coke formation and catalyst deactivation during bio-oil hydrodeoxygenation are thought to be primarily caused by the presence of phenolic compounds.[17,62] The oxygen functionalities in the phenolic compounds have the tendency to bond on the catalyst surface thereby accelerating the rate of deactivation.[14] From the results presented here, catalyst deactivation was evident, as the anisole conversion decreased with increasing number of reaction cycles, suggesting coke deposition or metal particle aggregation on the catalyst surface. Conversion dropped to 49.0% on the mic-Ni/ZSM-5 catalyst, from 92.1% recorded on the fresh catalyst. For hie-Ni/ZSM-5 and $Ni/SiO_2$ catalysts, conversion decreased from 100% and 92.4 to 72.0% and 50.0%, respectively. Compared to the mic-Ni/ZSM-5 and $Ni/SiO_2$ catalysts, the hie-Ni/ZSM-5 catalyst shows the best stability in terms of liquid product selectivity. Cyclohexane selectivity only changed from 88.1% to 91.9% with no other liquid product detected throughout the three reaction cycles. However, a small amount of toluene emerged in the product from the second and third hydrodeoxygenation reaction cycles over the mic-Ni/ZSM-5 catalyst. This implies a decrease in the demethoxylation ability of the catalyst owing to the low acidity which made part of the reactant transform via the isomerization−direct deoxygenation pathway.

The reusability test suggested improved metal dispersion on hie-Ni/ZSM-5 as explained in the previous section. Metal particles on the external surface of a catalyst are less stable than those within the zeolite pores; as such, the tendency of metal sintering and aggregation is high on the catalyst surface.[14,63] Recently, Pt/HZSM-5 was employed in the hydrodeoxygenation of levulinic acid at 200 °C and 10 bar hydrogen pressure. It was found that an increase in the number of Pt particles on the external surface of ZSM-5 negatively affects the turn over frequency of the pentanoic acid product due to the agglomeration of Pt during the reaction.[2] In addition to coke deposition and metal sintering, another major catalyst deactivation driver during the hydrodeoxygenation reaction is the solvent.[14,51,64] The extent of metal washing or leaching from a support depends on the type of solvent and conditions of the reaction as well as the nature of the metal−support interaction; potentially, a weak interaction leads to high metal loss. In this work, metal leaching from the three catalysts was insignificant as revealed by the EDX elemental mapping result, shown in Table S4; hence, coke might be one of the major


https://doi.org/10.1021/acs.energyfuels.2c03734
Energy Fuels XXXX, XXX, XXX−XXX

causes of the decrease in catalytic activity noticed. Therefore, thermogravimetric analysis (TGA) was performed on both the used and the fresh catalysts.

Figure 9 presents weight loss against temperature profiles for the fresh and used catalysts. This was recorded between 100

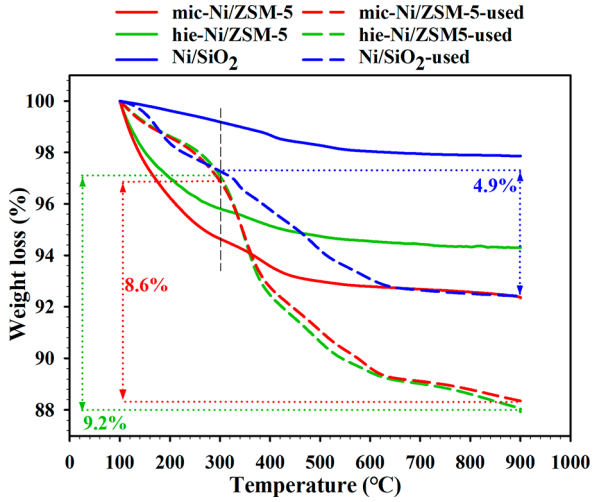


**Figure 9.** Thermogravimetric analysis (TGA) of fresh and used catalysts.

and 900 °C at a heating rate of 10 °C/min. Below 300 °C, weight loss was ascribed to water contents in the catalysts, and above 300 °C, loss was associated with the deposited coke on the catalysts surfaces during the hydrodeoxygenation reaction. The fresh $Ni/SiO_2$, mic-Ni/ZSM-5, and hie-Ni/ZSM-5 catalysts displayed weight losses of 0.8%, 5.4%, and 4.2% below 300 °C, respectively, on account of the desorption of adsorbed water. Above 300 °C, further losses of 1.4%, 2.2%, and 1.5% were recorded for the three catalysts. This weight loss could be linked to the presences of some organic residues in the catalysts.[45] Between 300 and 900 °C, weight losses of 8.6, 9.2, and 4.9 wt % were recorded on the spent mic-Ni/ZSM-5, hie-Ni/ZSM-5, and $Ni/SiO_2$ catalysts, respectively. This confirmed the accumulations of organic compounds on the surfaces of the catalysts. Noticeably, the $Ni/SiO_2$ catalyst with the highest density of strong acid sites and shortest life span has the lowest coke content. Although hie-Ni/ZSM-5 showed the largest amount of coke deposit, it demonstrated the highest activity and product selectivity in the catalyst reusability test. This result is in agreement with the observation of Ni et al.,[65] who reported superior catalytic activity over the Zn-Al/ZSM-5-T catalyst with the highest quantity of coke deposit compared with the Zn-Al/ZSM-5 catalyst during aromatization of methanol.

## 4. CONCLUSION

Nickel-based ZSM-5 and $SiO_2$ catalysts were prepared, characterized, and tested in the hydrodeoxygenation of anisole as bio-oil model compounds. Decreases in crystallinity and formation of mesopores after the parent ZSM-5 was treated with 0.2 M NaOH were seen from the XRD and BET results. $H_2$-TPR, $NH_3$-TPD, and TEM analyses revealed how metal dispersion on the support and metal−support interaction were greatly affected by the support nature. The variation seen in conversion and product distribution showed the influences of the support properties, particularly, porosity and acidity. Acidity of the support in combination with the active metal sites demonstrated a synergetic effect that favors the hydrodeoxygenation reaction of anisole. The catalytic activity increased with increasing reaction temperature and hydrogen partial pressure to the optimum at 200 °C and 60 bar. Changing the reaction solvent from decahydronaphthalene to *n*-decane did not show any noticeable difference in terms of anisole conversion and product distribution. The order of catalytic activity decreases as follows: hie-Ni/ZSM-5 > mic-Ni/ZSM-5 > $Ni/SiO_2$, with the highest anisole conversion of 100% in 120 min over the hie-Ni/ZSM-5 catalyst. A simplified reaction scheme proposed claimed the transformation of anisole proceeds via either a direct deoxygenation−hydrogenation or isomerization−direct deoxygenation route, with total hydrodeoxygenation on all the catalysts and complete hydrodearomatization on hie-Ni/ZSM-5, but only 84.6% over $Ni/SiO_2$. The dominant product on mic-Ni/ZSM-5 and hie-Ni/ZSM-5 catalysts was cyclohexane, whereas toluene was the major product from the $Ni/SiO_2$ catalyst. Notably, the catalyst reusability test revealed improved catalytic activity and very good stability in terms of liquid product selectivity over the hie-Ni/ZSM-5 catalyst. Hence, compared with the mic-ZSM-5 and $SiO_2$ supports, the 0.2 M NaOH-treated sample proved to be the best solid-support candidate.

## ■ ASSOCIATED CONTENT

### Supporting Information

The Supporting Information is available free of charge at https://pubs.acs.org/doi/10.1021/acs.energyfuels.2c03734.

Figure S1: SEM images of the catalyst supports. Figure S2: Deconvolution profiles of $NH_3$-TPD results for all supports and their corresponding catalysts. Figure S3: Additional information on the extent of hydrodeoxygenation (HDO %) and hydrodearomatization (HAD %) over the catalysts. Table S4: Elemental compositions of spent catalysts. (PDF)

## ■ AUTHOR INFORMATION


### Corresponding Author

**Joseph Wood** − *School of Chemical Engineering, University of Birmingham, Birmingham B15 2TT, United Kingdom;* orcid.org/0000-0003-2040-5497; Phone: +44(0)121 414 5295; Email: j.wood@bham.ac.uk

### Authors

**Mustapha Yusuf** − *School of Chemical Engineering, University of Birmingham, Birmingham B15 2TT, United Kingdom; Department of Chemical Engineering, Ahmadu Bello University, Zaria 810261, Nigeria*

**Gary Leeke** − *School of Chemical Engineering, University of Birmingham, Birmingham B15 2TT, United Kingdom*

Complete contact information is available at: https://pubs.acs.org/10.1021/acs.energyfuels.2c03734


### Notes

The authors declare no competing financial interest.

## ■ ACKNOWLEDGMENTS

The authors are grateful to the Petroleum Technology Development Fund (PTDF), Abuja, Nigeria, for financing the research. The following persons are highly appreciated: June Callison, Lisa Allen, and Sining Chen for their support

with access and training on ChemBET and CatLab at the Research Complex Harwell and Abubakar Muhammad, Oriyomi Ogunbanjo, and Musa Mahmud of the School of Chemistry for proving the XRD and SEM analyses.

## REFERENCES

(1) Berenguer, A.; Bennett, J. A.; Hunns, J.; Moreno, I.; Coronado, J. M.; Lee, A. F.; Pizarro, P.; Wilson, K.; Serrano, D. P. Catalytic Hydrodeoxygenation of M-Cresol over Ni2P/Hierarchical ZSM-5. *Catal. Today* **2018**, *304*, 72−79.

(2) Luo, W.; Cao, W.; Bruijnincx, P. C. A.; Lin, L.; Wang, A.; Zhang, T. Zeolite-Supported Metal Catalysts for Selective Hydrodeoxygenation of Biomass-Derived Platform Molecules. *Green Chem.* **2019**, *21* (14), 3744−3768.

(3) Oh, S.; Ahn, S. H.; Choi, J. W. Effect of Different Zeolite Supported Bifunctional Catalysts for Hydrodeoxygenation of Waste Wood Bio-Oil. *J. Korean Wood Sci. Technol.* **2019**, *47* (3), 344−359.

(4) Sankaranarayanan, T. M.; Kreider, M.; Berenguer, A.; Gutiérrez-Rubio, S.; Moreno, I.; Pizarro, P.; Coronado, J. M.; Serrano, D. P. Cross-Reactivity of Guaiacol and Propionic Acid Blends during Hydrodeoxygenation over Ni-Supported Catalysts. *Fuel* **2018**, *214*, 187−195.

(5) Hansen, S.; Mirkouei, A.; Diaz, L. A. A Comprehensive State-of-Technology Review for Upgrading Bio-Oil to Renewable or Blended Hydrocarbon Fuels. *Renew. Sustain. Energy Rev.* **2020**, *118*, 109548.

(6) Kim, H.; Yang, S.; Lim, Y. H.; Ha, J. M.; Kim, D. H. Upgrading Bio-Oil Model Compound over Bifunctional Ru/HZSM-5 Catalysts in Biphasic System: Complete Hydrodeoxygenation of Vanillin. *J. Hazard. Mater.* **2022**, *423* (PA), 126525.

(7) Witsuthammakul, A.; Sooknoi, T. Selective Hydrodeoxygenation of Bio-Oil Derived Products: Ketones to Olefins. *Catal. Sci. Technol.* **2015**, *5* (7), 3639−3648.

(8) Song, M.; Zhong, Z.; Dai, J. Different Solid Acid Catalysts Influence on Properties and Chemical Composition Change of Upgrading Bio-Oil. *J. Anal. Appl. Pyrolysis* **2010**, *89* (2), 166−170.

(9) Qu, L.; Jiang, X.; Zhang, Z.; Zhang, X. G.; Song, G. Y.; Wang, H. L.; Yuan, Y. P.; Chang, Y. L. A Review of Hydrodeoxygenation of Bio-Oil: Model Compounds, Catalysts, and Equipment. *Green Chem.* **2021**, *23* (23), 9348−9376.

(10) Tang, X.; Ding, W.; Li, H. Improved Hydrodeoxygenation of Bio-Oil Model Compounds with Polymethylhydrosiloxane by Brønsted Acidic Zeolites. *Fuel* **2021**, *290*, 119883.

(11) Niu, X.; Feng, F.; Yuan, G.; Zhang, X.; Wang, Q. Hollow MFI Zeolite Supported Pt Catalysts for Highly Selective and Stable Hydrodeoxygenation of Guaiacol to Cycloalkanes. *Nanomaterials* **2019**, *9* (3), 362.

(12) Mortensen, P. M.; Grunwaldt, J. D.; Jensen, P. A.; Knudsen, K. G.; Jensen, A. D. A Review of Catalytic Upgrading of Bio-Oil to Engine Fuels. *Appl. Catal. A Gen.* **2011**, *407* (1−2), 1−19.

(13) Pawelec, B.; Loricera, C. V.; Geantet, C.; Mota, N.; Fierro, J. L. G.; Navarro, R. M. Factors Influencing Selectivity in the Liquid-Phase Phenol Hydrodeoxygenation over ZSM-5 Supported Pt/Ir and Pt+Ir Catalysts. *Mol. Catal.* **2020**, *482*, 110669.

(14) Tu, C.; Chen, J.; Li, W.; Wang, H.; Deng, K.; Vinokurov, V. A.; Huang, W. Hydrodeoxygenation of Bio-Derived Anisole to Cyclohexane over Bi-Functional IM-5 Zeolite Supported Ni Catalysts. *Sustain. Energy Fuels* **2019**, *3* (12), 3462−3472.

(15) Gutiérrez-Rubio, S.; Moreno, I.; Serrano, D. P.; Coronado, J. M. Hydrotreating of Guaiacol and Acetic Acid Blends over Ni2P/ZSM-5 Catalysts: Elucidating Molecular Interactions during Bio-Oil Upgrading. *ACS Omega* **2019**, *4* (25), 21516−21528.

(16) Keav, S.; Martin, A.; Barbier, J.; Duprez, D. Deactivation and Reactivation of Noble Metal Catalysts Tested in the Catalytic Wet Air Oxidation of Phenol. *Catal. Today* **2010**, *151* (1−2), 143−147.

(17) Gao, D.; Schweitzer, C.; Hwang, H. T.; Varma, A. Conversion of Guaiacol on Noble Metal Catalysts: Reaction Performance and Deactivation Studies. *Ind. Eng. Chem. Res.* **2014**, *53* (49), 18658−18667.

(18) Zhang, Y.; Wu, S.; Xu, X.; Jiang, H. Ethane Aromatization and Evolution of Carbon Deposits over Nanosized and Microsized Zn/ZSM-5 Catalysts. *Catal. Sci. Technol.* **2020**, *10* (3), 835−843.

(19) Zhao, H.; Hu, X.; Hao, J.; Li, N.; Zhi, K.; He, R.; Wang, Y.; Zhou, H.; Liu, Q. An Efficient Bifunctional Ru-NbOPO4 Catalyst for the Hydrodeoxygenation of Aromatic Ethers, Phenols and Real Bio-Oil. *Appl. Catal. A Gen.* **2020**, *591*, 117378.

(20) Chaihad, N.; Karnjanakom, S.; Kurnia, I.; Yoshida, A.; Abudula, A.; Reubroycharoen, P.; Guan, G. Catalytic Upgrading of Bio-Oils over High Alumina Zeolites. *Renew. Energy* **2019**, *136*, 1304−1310.

(21) Lawal, A. M.; Hart, A.; Daly, H.; Hardacre, C.; Wood, J. Catalytic Hydrogenation of Short Chain Carboxylic Acids Typical of Model Compound Found in Bio-Oils. *Ind. Eng. Chem. Res.* **2019**, *58* (19), 7998−8008.

(22) Liu, L. J.; Liu, Y. G.; Gao, X.; Zhang, R. Q.; Zhai, Y. P. Hydrodeoxygenation of Bio-Oil Model Compounds over Amorphous NiB/SiO2-Al2O3 Catalyst in Oil-Water Biphasic System. *Ranliao Huaxue Xuebao/Journal Fuel Chem. Technol.* **2017**, *45* (8), 932−938.

(23) Zhang, X.; Long, J.; Kong, W.; Zhang, Q.; Chen, L.; Wang, T.; Ma, L.; Li, Y. Catalytic Upgrading of Bio-Oil over Ni-Based Catalysts Supported on Mixed Oxides. *Energy Fuels* **2014**, *28* (4), 2562−2570.

(24) Zhao, T.; Wang, Y.; Sun, C.; Zhao, A.; Wang, C.; Zhang, X.; Zhao, J.; Wang, Z.; Lu, J.; Wu, S.; Liu, W. Direct Synthesis of Hierarchical Binder-Free ZSM-5 and Catalytic Properties for MTP. *Microporous Mesoporous Mater.* **2020**, *292*, 109731.

(25) Li, X.; Chen, G.; Liu, C.; Ma, W.; Yan, B.; Zhang, J. Hydrodeoxygenation of Lignin-Derived Bio-Oil Using Molecular Sieves Supported Metal Catalysts: A Critical Review. *Renew. Sustain. Energy Rev.* **2017**, *71*, 296−308.

(26) Saidi, M.; Safaripour, M. Aqueous Phase Hydrodeoxygenation of Anisole as a Pyrolysis Lignin-Derived Bio-Oil by Ether-Functionalized Ionic Polymer-Stabilized Ni-Mo Nanocatalyst. *Sustain. Energy Technol. Assessments* **2022**, *49*, 101770.

(27) Ma, Z.; Wei, L.; Zhou, W.; Jia, L.; Hou, B.; Li, D.; Zhao, Y. Upgrading of Fast Pyrolysis Bio-Oil to Drop-in Fuel over Ru Catalysts. *J. Energy Inst.* **2019**, *92* (4), 855−860.

(28) Szczyglewska, P.; Feliczak-Guzik, A.; Nowak, I. A Support Effect on the Hydrodeoxygenation Reaction of Anisole by Ruthenium Catalysts. *Microporous Mesoporous Mater.* **2020**, *293*, 109771.

(29) Nesterov, N. S.; Smirnov, A. A.; Pakharukova, V. P.; Yakovlev, V. A.; Martyanov, O. N. Advanced Green Approaches for the Synthesis of NiCu-Containing Catalysts for the Hydrodeoxygenation of Anisole. *Catal. Today* **2021**, *379*, 262−271.

(30) Li, W.; Li, F.; Wang, H.; Liao, M.; Li, P.; Zheng, J.; Tu, C.; Li, R. Hierarchical Mesoporous ZSM-5 Supported Nickel Catalyst for the Catalytic Hydrodeoxygenation of Anisole to Cyclohexane. *Mol. Catal.* **2020**, *480*, 110642.

(31) Li, W.; Wang, H.; Wu, X.; Betancourt, L. E.; Tu, C.; Liao, M.; Cui, X.; Li, F.; Zheng, J.; Li, R. Ni/Hierarchical ZSM-5 Zeolites as Promising Systems for Phenolic Bio-Oil Upgrading: Guaiacol Hydrodeoxygenation. *Fuel* **2020**, *274*, 117859.

(32) Bhoi, P. R.; Ouedraogo, A. S.; Soloiu, V.; Quirino, R. Recent Advances on Catalysts for Improving Hydrocarbon Compounds in Bio-Oil of Biomass Catalytic Pyrolysis. *Renew. Sustain. Energy Rev.* **2020**, *121*, 109676.

(33) Yan, P.; Kennedy, E.; Stockenhuber, M. Natural Zeolite Supported Ni Catalysts for Hydrodeoxygenation of Anisole. *Green Chem.* **2021**, *23* (13), 4673−4684.

(34) Rac, V.; Rakíc, V.; Miladinovíc, Z.; Stošić, D.; Auroux, A. Influence of the Desilication Process on the Acidity of HZSM-5 Zeolite. *Thermochim. Acta* **2013**, *567*, 73−78.

(35) Osatiashtiani, A.; Puértolas, B.; Oliveira, C. C. S.; Manayil, J. C.; Barbero, B.; Isaacs, M.; Michailof, C.; Heracleous, E.; Pérez-Ramírez, J.; Lee, A. F.; Wilson, K. On the Influence of Si:Al Ratio and Hierarchical Porosity of FAU Zeolites in Solid Acid Catalysed Esterification Pretreatment of Bio-Oil. *Biomass Convers. Biorefinery* **2017**, *7* (3), 331−342.

(36) Dauda, I. B.; Yusuf, M.; Gbadamasi, S.; Bello, M.; Atta, A. Y.; Aderemi, B. O.; Jibril, B. Y. Highly Selective Hierarchical ZnO/ZSM-



https://doi.org/10.1021/acs.energyfuels.2c03734
Energy Fuels XXXX, XXX, XXX−XXX

5 Catalysts for Propane Aromatization. *ACS Omega* **2020**, *5*, 2725−2733.
(37) Lee, K.; Yoo, K. S. Kinetics and Optimization of Dimethyl Carbonate Synthesis by Transesterification Using Design of Experiment. *Korean Chem. Eng. Res.* **2018**, *56* (3), 416−420.
(38) Moersidik, S. S.; Nugroho, R.; Handayani, M.; Kamilawati; Pratama, M. A. Optimization and Reaction Kinetics on the Removal of Nickel and COD from Wastewater from Electroplating Industry Using Electrocoagulation and Advanced Oxidation Processes. *Heliyon* **2020**, *6* (2), e03319.
(39) Li, M.; Zhao, H.; Lu, Z. Y. Porphyrin-Based Porous Organic Polymer, Py-POP, as a Multifunctional Platform for Efficient Selective Adsorption and Photocatalytic Degradation of Cationic Dyes. *Microporous Mesoporous Mater.* **2020**, *292*, 109774.
(40) Chen, G.; Liu, J.; Li, X.; Zhang, J.; Yin, H.; Su, Z. Investigation on Catalytic Hydrodeoxygenation of Eugenol Blend with Light Fraction in Bio-Oil over Ni-Based Catalysts. *Renew. Energy* **2020**, *157*, 456−465.
(41) Lestari, A. R.; Suratmo; Ulfa, S. M. Effect of Support on the Hydrodeoxygenation of Phenol Using Ni-Based Metal Catalysts: Ni/$SiO_2$, Ni/$ZrO_2$, and Ni/$Al_2O_3$. *IOP Conf. Ser. Mater. Sci. Eng.* **2019**, *546* (7), 072004.
(42) Lovell, E. C.; Scott, J.; Amal, R. Ni-SiO2 Catalysts for the Carbon Dioxide Reforming of Methane: Varying Support Properties by Flame Spray Pyrolysis. *Molecules* **2015**, *20* (3), 4594−4609.
(43) Al Soubaihi, R. M.; Saoud, K. M.; Ye, F.; Zar Myint, M. T.; Saeed, S.; Dutta, J. Synthesis of Hierarchically Porous Silica Aerogel Supported Palladium Catalyst for Low-Temperature CO Oxidation under Ignition/Extinction Conditions. *Microporous Mesoporous Mater.* **2020**, *292*, 109758.
(44) Sankaranarayanan, T. M.; Berenguer, A.; Ochoa-Hernández, C.; Moreno, I.; Jana, P.; Coronado, J. M.; Serrano, D. P.; Pizarro, P. Hydrodeoxygenation of Anisole as Bio-Oil Model Compound over Supported Ni and Co Catalysts: Effect of Metal and Support Properties. *Catal. Today* **2015**, *243* (C), 163−172.
(45) Sadowska, K.; Wach, A.; Olejniczak, Z.; Kuśtrowski, P.; Datka, J. Hierarchic Zeolites: Zeolite ZSM-5 Desilicated with NaOH and NaOH/Tetrabutylamine Hydroxide. *Microporous Mesoporous Mater.* **2013**, *167*, 82−88.
(46) Serrano, D. P.; Aguado, J.; Escola, J. M.; Peral, A.; Morales, G.; Abella, E. Synthesis of Hierarchical ZSM-5 by Silanization and Alkoxylation of Protozeolitic Units. *Catal. Today* **2011**, *168* (1), 86−95.
(47) Ghampson, I. T.; Sepúlveda, C.; Dongil, A. B.; Pecchi, G.; García, R.; Fierro, J. L. G.; Escalona, N. Phenol Hydrodeoxygenation: Effect of Support and Re Promoter on the Reactivity of Co Catalysts. *Catal. Sci. Technol.* **2016**, *6* (19), 7289−7306.
(48) You, S. J.; Park, E. D. Effects of Dealumination and Desilication of H-ZSM-5 on Xylose Dehydration. *Microporous Mesoporous Mater.* **2014**, *186*, 121−129.
(49) Gamliel, D. P.; Baillie, B. P.; Augustine, E.; Hall, J.; Bollas, G. M.; Valla, J. A. Nickel Impregnated Mesoporous USY Zeolites for Hydrodeoxygenation of Anisole. *Microporous Mesoporous Mater.* **2018**, *261*, 18−28.
(50) He, L.; Xin, Z.; Gao, W.; Gu, J.; Meng, X. Highly Efficient Porous Ni/SiO2 Catalysts Prepared by Electrospinning Method for CO Methanation. *Huagong Xuebao/CIESC J.* **2020**, *71* (11), 5007−5015.
(51) Gorzin, F.; Yaripour, F. Production of Light Olefins from Methanol over Modified H-ZSM-5: Effect of Metal Impregnation in High-Silica Zeolite on Product Distribution. *Res. Chem. Intermed.* **2019**, *45* (2), 261−285.
(52) Feng, D.; Feng, Y.; Li, P.; Zang, Y.; Wang, C.; Zhang, X. Modified Mesoporous Silica Filled with PEG as a Shape-Stabilized Phase Change Materials for Improved Thermal Energy Storage Performance. *Microporous Mesoporous Mater.* **2020**, *292*, 109756.
(53) Yang, W.; Wang, Z.; Song, S.; Chen, H.; Wang, X.; Cheng, J.; Sun, R.; Han, J. Understanding Catalytic Mechanisms of HZSM-5 in Hydrothermal Liquefaction of Algae through Model Components: Glucose and Glutamic Acid. *Biomass and Bioenergy* **2019**, *130*, 105356.
(54) Feng, R.; Yan, X.; Hu, X.; Wang, Y.; Li, Z.; Hou, K.; Lin, J. Hierarchical ZSM-5 Zeolite Designed by Combining Desilication and Dealumination with Related Study of n-Heptane Cracking Performance. *J. Porous Mater.* **2018**, *25* (6), 1743−1756.
(55) Li, K.; Wang, R.; Chen, J. Hydrodeoxygenation of Anisole over Silica-Supported Ni2P, MoP, and NiMoP Catalysts. *Energy Fuels* **2011**, *25* (3), 854−863.
(56) Li, F. X.; Wang, X. F.; Zheng, Y.; Chen, J. X. Influence of Metallic Promoters on the Performance of Ni/SiO2 Catalyst in the Hydrodeoxygenation of Anisole. *Ranliao Huaxue Xuebao/Journal Fuel Chem. Technol.* **2018**, *46* (1), 75−83.
(57) Li, Z.; Jiang, E.; Xu, X.; Sun, Y.; Tu, R. Hydrodeoxygenation of Phenols, Acids, and Ketones as Model Bio-Oil for Hydrocarbon Fuel over Ni-Based Catalysts Modified by Al, La and Ga. *Renew. Energy* **2020**, *146*, 1991−2007.
(58) Ghampson, I. T.; Canales, R.; Escalona, N. A Study of the Hydrodeoxygenation of Anisole over Re-MoOx/TiO2 Catalyst. *Appl. Catal. A Gen.* **2018**, *549*, 225−236.
(59) Li, W.; Li, F.; Wang, H.; Liao, M.; Li, P.; Zheng, J.; Tu, C.; Li, R. Hierarchical Mesoporous ZSM-5 Supported Nickel Catalyst for the Catalytic Hydrodeoxygenation of Anisole to Cyclohexane. *Mol. Catal.* **2020**, *480*, 110642.
(60) Tu, C.; Chen, J.; Li, W.; Wang, H.; Deng, K.; Vinokurov, V. A.; Huang, W. Hydrodeoxygenation of Bio-Derived Anisole to Cyclohexane over Bi-Functional IM-5 Zeolite Supported Ni Catalysts. *Sustain. Energy Fuels* **2019**, *3* (12), 3462−3472.
(61) Yan, P.; Tian, X.; Kennedy, E. M.; Stockenhuber, M. The Role of Ni Sites Located in Mesopores in the Selectivity of Anisole Hydrodeoxygenation. *Catal. Sci. Technol.* **2022**, *12* (7), 2184−2196.
(62) Si, Z.; Zhang, X.; Wang, C.; Ma, L.; Dong, R. An Overview on Catalytic Hydrodeoxygenation of Pyrolysis Oil and Its Model Compounds. *Catalysts* **2017**, *7* (6), 169.
(63) Kumar, A.; Kumar, A.; Biswas, B.; Kumar, J.; Yenumala, S. R.; Bhaskar, T. Hydrodeoxygenation of M-Cresol over Ru Based Catalysts: Influence of Catalyst Support on m-Cresol Conversion and Methylcyclohexane Selectivity. *Renew. Energy* **2020**, *151*, 687−697.
(64) Ding, Y. L.; Wang, H. Q.; Xiang, M.; Yu, P.; Li, R. Q.; Ke, Q. P. The Effect of Ni-ZSM-5 Catalysts on Catalytic Pyrolysis and Hydro-Pyrolysis of Biomass. *Front. Chem.* **2020**, *8*, 1−11.
(65) Ni, Y.; Sun, A.; Wu, X.; Hai, G.; Hu, J.; Li, T.; Li, G. The Preparation of Nano-Sized H[Zn, Al]ZSM-5 Zeolite and Its Application in the Aromatization of Methanol. *Microporous Mesoporous Mater.* **2011**, *143* (2−3), 435−442.


https://doi.org/10.1021/acs.energyfuels.2c03734
Energy Fuels XXXX, XXX, XXX−XXX